Electronic Supplementary Material (ESI) for Journal of Materials Chemistry A.

Electronic Supporting Information

Metal-organic frameworks derived hollow NiS_2 spheres encased in graphene layers for enhanced sodium-ion storage

Ran Bi,[ab] Cheng Zeng,[b] Huawen Huang,[b] Xinping Wang*[a] and Lei Zhang*[bc]

[a]State Key Laboratory of Fine Chemical, School of Environmental Science and Technology, Dalian University of Technology, Dalian 116024, P. R. China

Email: dllgwxp@dlut.edu.cn

[b]Key Lab of Heat Transfer Enhancement and Energy Conservation of Ministry of Education, School of Chemistry & Chemical Engineering, South China University of Technology, Guangzhou 510640, P. R. China

E-mail: celeizhang@scut.edu.cn

[c]Key Lab of Advanced Energy Materials Chemistry (Ministry of Education), Nankai University, Tianjin 300071, P. R. China

Experimental section

Materials Synthesis

Synthesis of Ni-MOFs

As reported previously,[1] 432.0 mg of $Ni(NO_3)_2\cdot 6H_2O$, 1.5 g of PVP (Mw=40000) and 150.0 of mg trimesic acid (H_3BTC) were dissolved in a 30 mL of mixture solution (volume ratio of Water:Ethanol:DMF is 1:1:1). After vigorous stirring for 40 min, the uniform light green solution was transferred into a 50 mL Teflon-lined stainless-steel autoclave and heated to 150 ^oC for 15 h. The green products were collected by centrifugation at 4400 rpm for 10 min, washed with ethanol for 3 times and dried at 60 ^oC for 8 h, giving hollow Ni-MOFs spheres. Solid Ni-MOFs spheres were obtained by reducing the hydrothermal reaction time to 3 h.

Synthesis of hollow NiS_2@G and porous NiS_2@C spheres.

The hollow NiS_2@G spheres were synthesized by a one-step thermal treatment involving simultaneous carbonization and sulfidation. Typically, 80.0 mg of as-synthesized hollow Ni-MOFs spheres and 100.0 mg of sulfur powder were placed at two separate positions in a quartz boat with sulfur powder at the upstream side. The samples were then heated to 450 ^oC for 2 h under N_2 atmosphere with a heating ramp of 1 $^oC\ min^{-1}$. The furnace was subsequently cooled down to room temperature to obtain hollow NiS_2@G spheres. For comparison, porous NiS_2@C spheres were also synthesized by using solid Ni-MOFs spheres as processor through the similar calcination procedure.

Material Characterizations

Scanning electron microscopy (SEM) images were obtained by SU8220 operated at 10 kV. The transmission electron microscope (TEM) images and the high-resolution transmission electron microscope (HRTEM) images were taken on JEOL JEM 2100F. X-ray diffraction (XRD) patterns were recorded with a Bruker D8 Advance with Cu Kα radiation at 35 kV and 15 mA. Thermogravimetric analysis (TGA) was carried out using Netzsch STA449F5 under air flow from room temperature to 800 °C with a heating ramp of 10 °C min^{-1}. The specific surface area and pore size distribution were conducted on the nitrogen adsorption-desorption instrument (Micromeritics 3Flex) based on Brunauer-Emmett-Teller (BET) multipoint method and Barret-Joyner-Halenda (BJH) model, respectively. Raman spectrum was collected on LabRAM Aramis with a laser wavelength of 532 nm.

Electrochemical Measurements

The electrode slurry was prepared by mixing active materials, Super P and PVDF (polyvinylidene fluoride dissolved in N-Methyl pyrrolidone) in a weight ratio of 6:3:1. The mixture was then cast on a copper foil and dried in a vacuum oven at 60 °C overnight. The loading mass of the electrode materials is around 1.0 mg cm^{-2}. The working electrode was punched into disks with a diameter of 12 mm by a hollow punch. The 2032 coin cells were assembled in an argon-filled glovebox (H_2O and O_2 content below 0.1 ppm). Sodium metal foil and glass fiber GF/D (Whatman) were used as the counter electrode and the separator, respectively. The electrolyte is 1.0 M $NaPF_6$ in diglyme. The electrochemical performance at various current densities was tested using Neware battery testing system within the voltage range of 0.05−3 V. The cyclic voltammograms (CV) were recorded by a GAMRY electrochemical workstation at a scan rate of 0.1 mV s^{-1} at room temperature.

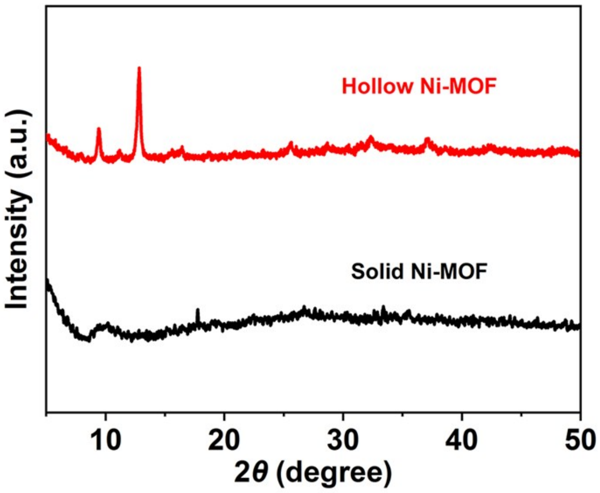

Fig. S1 XRD patterns of hollow Ni-MOFs and solid Ni-MOFs spheres.

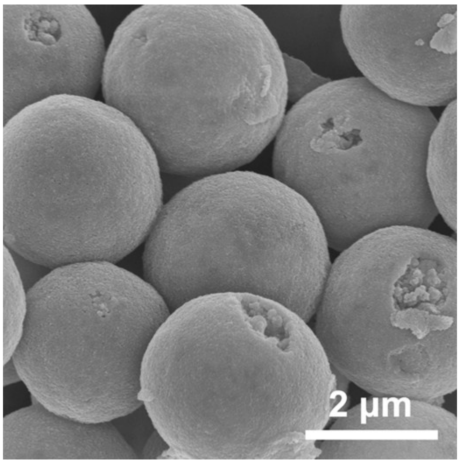

Fig. S2 SEM image of porous NiS_2@C spheres.

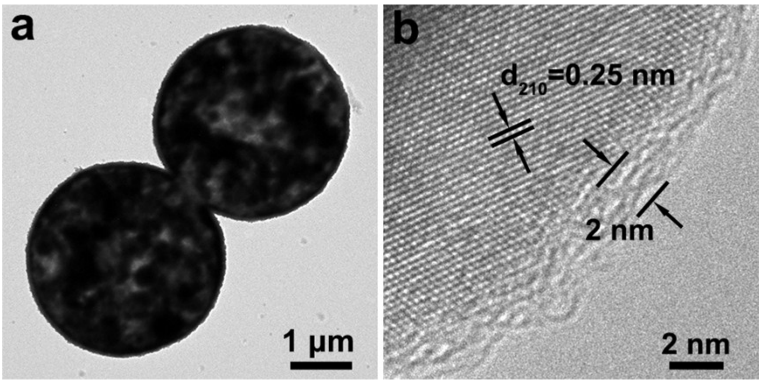

Fig. S3 TEM and HRTEM images of porous NiS_2@C spheres.

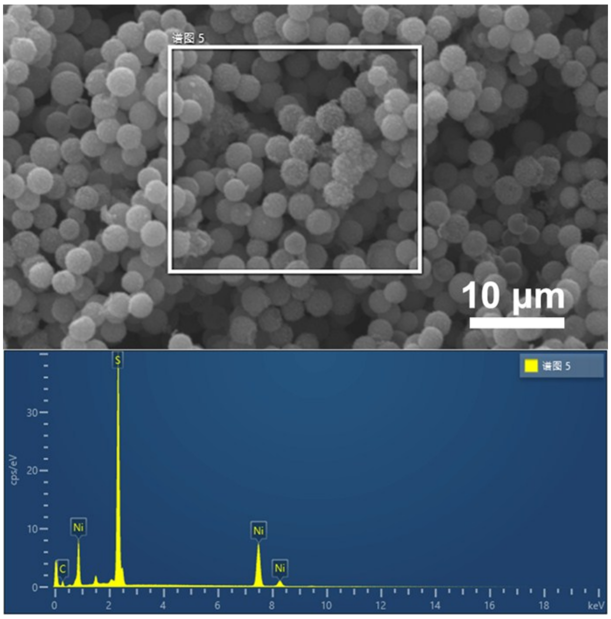

Elements	Weight %	Atomic %
C	23.51	51.56
S	37.90	31.13
Ni	38.59	17.31

Fig. S4 SEM image and EDS of hollow NiS_2@G spheres.

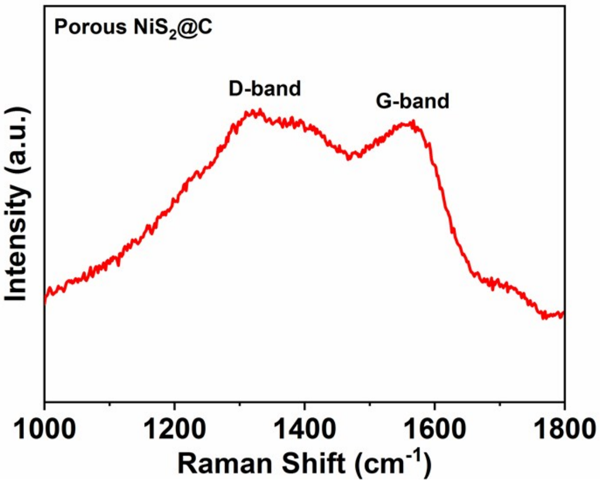

Fig. S5 Raman spectrum of porous NiS_2@C spheres.

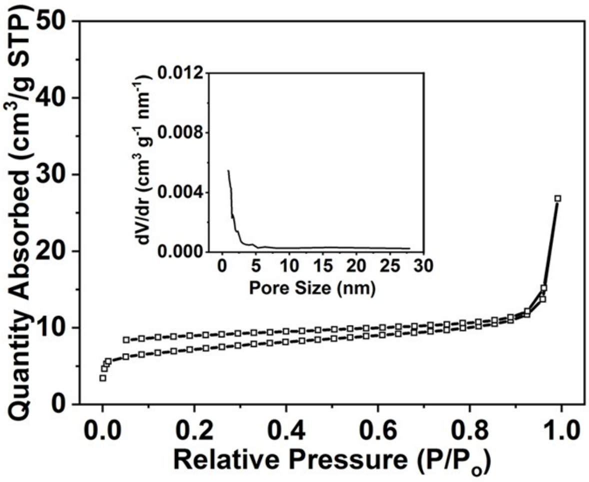

Fig. S6 Nitrogen adsorption−desorption isotherm of porous NiS_2@C spheres (the inset showing the pore size distribution). The unclosed desorption branch indicates irreversibility of nitrogen adsorption that nitrogen molecules are possibly trapped in small micropores in desorption process.

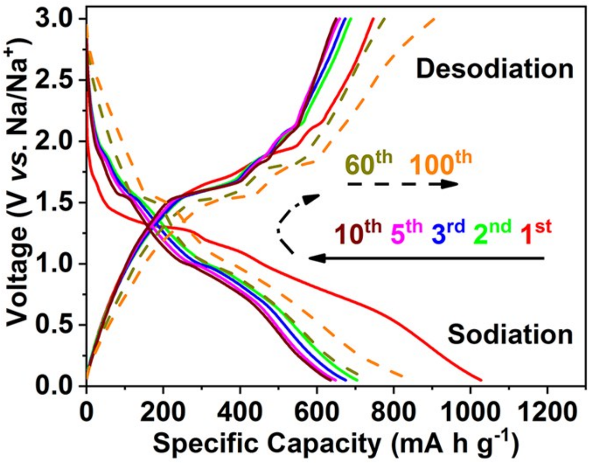

Fig. S7 Galvanostatic discharge and charge curves of hollow NiS_2@G spheres.

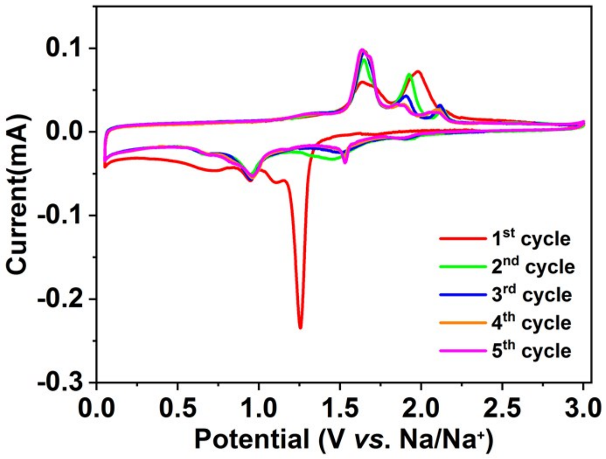

Fig. S8 CV curves of porous NiS_2@C spheres.

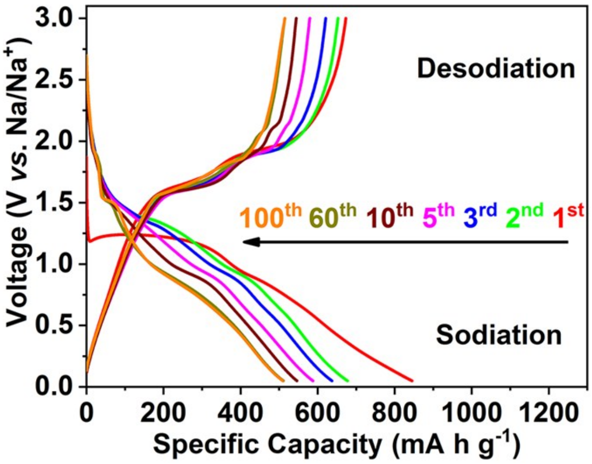

Fig. S9 Discharge and charge curves of porous NiS_2@C spheres.

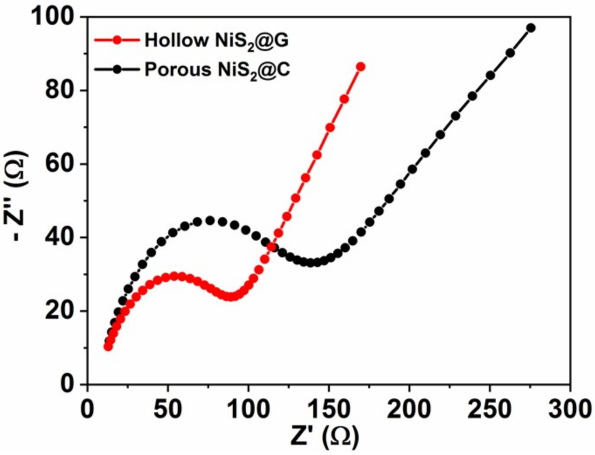

Fig. S10 Impedance spectra of the hollow NiS_2@G and porous NiS_2@C electrode after 100 cycles.

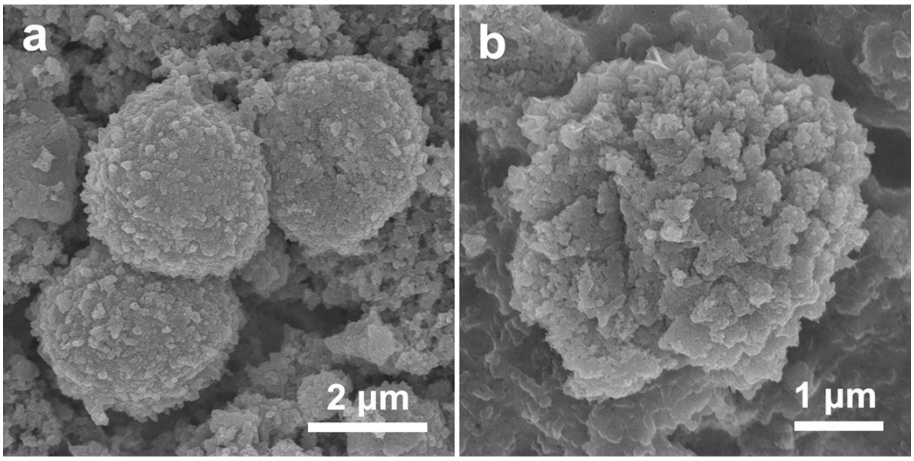

Fig. S11 SEM images of hollow NiS_2@G electrode after (a) 100 cycles and (b) 300 cycles.

Table S1. Summary and comparison of nickel sulfides-based materials as anode for SIBs

Materials	Weight content of NiS_x	Rate performance		Cycling performance		Ref.
		Capacity (mA h g^{-1})	Current (A g^{-1})	low current	high current	
Hollow NiS_2@G sphere	**83%**	**634.2, 585.4, 569.4, 549.5 and 527.8**	**0.1, 0.2, 0.5, 1 and 2**	**848 mA h g^{-1} after 100 cycles at 0.1 A g^{-1}**	**530 mA h g^{-1} after 300 cycles at 1 A g^{-1}**	**This work**
NiS_2-GNC	50%	382, 375, 325, 278 and 168	0.087, 0.16, 0.43, 0.87 and 1.6	313 mA h g^{-1} after 200 cycles at 0.087 A g^{-1}	-	2
NiS_2/C	~56%	397.4, 330.6, 290.5, 252.7 and 209.8	0.05, 0.1, 0.2, 0.3 and 0.5	280.6 mA h g^{-1} after 60 cycles at 0.1 A g^{-1}	186.9 mA h g^{-1} after 100 cycles at 0.5 A g^{-1}	3
NiS_2/NC	74.3%	528.3, 513.4, 452.2, 410.1, 343.5 and 294.4	0.1, 0.5, 1, 1.5, 2 and 3	505.7 mA h g^{-1} after 100 cycles at 0.1 A g^{-1}	356.2 mA h g^{-1} after 300 cycles at 0.5 A g^{-1}	4
NiS_2 nanosphere	-	681, 490, 420 and 253	0.3, 1.0, 2.0 and 5.0	About 450 mA h g^{-1} after 100 cycles at 0.1 A g^{-1}	319 mA h g^{-1} after 1000 cycles at 0.5 A g^{-1}	5
NiS_2/PCF	38.3%	580, 516, 450, 391, 347, 302 and 245	0.087, 0.16, 0.43, 0.87, 1.6, 4.3 and 8.7	561 mA h g^{-1} after 300 cycles at 0.087 A g^{-1}	275 mA h g^{-1} after 5000 cycles at 4.3 A g^{-1}	6
NiS_x-rGOS	-	515, 499, 477, 448 and 414	0.2, 0.5, 1.0, 2.0 and 4.0	516 mA h g^{-1} after 100 cycles at 0.2 A g^{-1}	-	7
Ni_3S_2/C	78.2%	583 to 529, 491, 459, 421 and 408	0.1 to 0.2, 0.4, 0.8, 1.6 and 2.0	453 mA h g^{-1} after 100 cycles at 0.1 A g^{-1}	408.2 mA h g^{-1} after 200 cycles at 2 A g^{-1}	8
Ni_3S_4/rGO	88.2%	310	4	630 mA h g^{-1} after 100 cycles at 0.05A g^{-1}	460 mA h g^{-1} after 200 cycles at 1 A g^{-1}	9

References

1. F. Zou, Y. M. Chen, K. Liu, Z. Yu, W. Liang, S. M. Bhaway, M. Gao and Y. Zhu, *ACS Nano*, 2016, **10**, 377−386.
2. T. Wang, P. Hu, C. Zhang, H. Du, Z. Zhang, X. Wang, S. Chen, J. Xiong and G. Cui, *ACS Appl. Mater. Interfaces*, 2016, **8**, 7811−7817.
3. K. J. Zhu, G. Liu, Y. J. Wang, J. Liu, S. T. Li, L. Y. Yang, S. L. Liu, H. Wang and T. Xie, *Mater. Lett.*, 2017, **197**, 180−183.
4. J. Li, J. Li, D. Yan, S. Hou, X. Xu, T. Lu, Y. Yao, W. Mai and L. Pan, *J. Mater. Chem. A*, 2018, **6**, 6595−6605.
5. R. Sun, S. Liu, Q. Wei, J. Sheng, S. Zhu, Q. An and L. Mai, *Small*, 2017, **13**, 1701744.
6. Q. Chen, S. Sun, T. Zhai, M. Yang, X. Zhao and H. Xia, *Adv. Energy Mater.*, 2018, **8**, 1800054.
7. H. Tao, M. Zhou, K. Wang, S. Cheng and J. Kai, *J. Mater. Chem. A*, 2017, **5**, 9322−9328.
8. X. Zhao, H. E. Wang, R. C. Massé, J. Cao, J. Sui, J. Li, W. Cai and G. Cao, *J. Mater. Chem. A*, 2017, **5**, 7394−7402.
9. J. Deng, Q. Gong, H. Ye, K. Feng, J. Zhou, C. Zha, J. Wu, J. Chen, J. Zhong and Y. Li, *ACS Nano*, 2018, **12**, 1829−1836.